An Implantable Wireless Network of Distributed Microscale Sensors for Neural Applications

Jihun Lee[1], Ethan Mok[1], Jiannan Huang[2], Lingxiao Cui[2], Ah-Hyoung Lee[3], Vincent Leung[2], Patrick Mercier[2], Steven Shellhammer[4], Lawrence Larson[1], Peter Asbeck[2], Ramesh Rao[2], Yoon-Kyu Song[3], Arto Nurmikko[1]*, and Farah Laiwalla[1]*

Abstract— **A vastly enhanced capability to bi-directionally interface with cortical microcircuits in a clinically viable way is the ultimate aspiration in neuroengineering. This necessitates a paradigm shift in neural interface system design beyond current bulky, monolithic constructs which are challenging to scale past 100-200 channels due to anatomic and engineering design constraints. A neural interface system relying on a spatially-distributed network of wireless microscale implantable sensors offers a highly scalable, robust and adaptive architecture for next-generation neural interfaces. We describe the development of a wireless network of sub-mm, untethered, individually addressable, fully wireless "Neurograin" sensors, in the context of an epicortical implant. Individual neurograin chiplets integrate a ~ 1 GHz wireless link for energy harvesting and telemetry with analog and digital electronics for neural signal amplification, on-chip storage, and networked communications via a TDMA protocol. Each neurograin thus forms a completely self-contained single channel of neural access and is implantable after post-process atomic layer deposition of thin-film (100 nm thick) barriers for hermetic sealing. Finally, ensembles of implantable neurograins form a fully wireless cortico-computer communication network (utilizing their unique device IDs). The implanted network is coordinated by a compact external "Epidermal Skinpatch" RF transceiver and data processing hub, which is implemented as a wearable module in order to be compatible with clinical implant considerations. We describe neurograin performance specifications and proof-of-concept in bench top and *ex vivo* and *in vivo* rodent platforms.**

I. INTRODUCTION

The development of chronic multi-channel recording methodologies such as Electrocorticography (ECoG) and multielectrode arrays (MEAs) over the last few decades, and the more recent integration of active electronics and wireless telemetry on these platforms has paved the way for robust, chronic research and clinical implantable brain-computer interfaces (BCIs) [1, 2]. The holy grail of BCI research is a real-time, closed-loop neural interface for complex, naturalistic tasks. This is only possible with a high spatial and temporal resolution sampling of neural activity with real-time feedback, across a multitude of cortical areas. The latter is challenging to implement at scales beyond 100-200 channels using currently available bulky monolithic implantable constructs. Scalability to thousands or tens of thousands of bidirectional neural interfacing nodes is the next frontier for

neuroengineering, and small distributed sensors have recently been proposed as one way to address this challenge [3]. A distributed sensor system is conceptually promising, so long as the individual sensor node is ultra-miniaturized to minimize volume overhead while maintaining a high-fidelity neural interface. It is then possible to envision a "cortical internet", comprising spatially-distributed clusters of sensors and actuators, providing bidirectional access to cortical neural networks from widespread brain areas in an adaptive fashion. We describe the development and testing validation from an epi-cortical implementation of this architecture, which we refer to as the "Neurograin" system. To the authors' best knowledge at the time of this writing, this represents the first reported demonstration of a completely wireless network of sensors in a neural application.

The neurograin system constitutes ensembles of implantable, sub-millimeter, individually addressable, microelectronic chiplets. Each neurograin is designed as a self-contained, hermetically sealed module measuring 500 µm x 500 µm x 35 µm, and powered through transcutaneous wireless power delivery via near-field inductive coupling at approximately 1 GHz. This activates on-chip electronics for neural signal transduction (ECoG signals with up to 500 Hz bandwidth in this epi-cortical application), on-chip memory storage and subsequent uplink telemetry via RF backscattering at 10 Mbps in accordance with the implemented time-domain multiple access (TDMA) network protocol. Our network communication protocol is currently designed to accommodate up to 1000 channels of broadband ECoG data in this prototype system, but extendable via parallelization and other techniques to 10 – 100x higher channel counts with compatible hardware changes. Neurograin microdevices can be individually or collectively implanted (latter e.g an ECoG grid or peripheral nerve cuff electrode) into selected areas of the brain or peripheral nervous system (PNS), thereby forming untethered, broadband, bidirectional neural interfacing elements usable for a variety of diagnostic and therapeutic neural applications.

The remainder of this paper is organized as follows: *Section II* describes components of the Neurograin System Design, *Section III* reports on bench top testing and validation of Neurograin performance at the level of single as well as

small ensembles of Neurograins, and *Section IV* illustrates results from physiologic recordings from *ex vivo* and *in vivo* rodent test beds. Finally, *Section V* summarizes these novel contributions and future directions in the context of the BCI application space.

II. SYSTEM DESIGN

Scalability and implantability are the two primary drivers dictating the neurograin system architecture. As such, we have taken an aggressive approach to scaling down implant volume, with individual neurograin chiplet size being 0.00675 mm³ (including the hermetic barrier) in the current implementation. While this is already > 10-100x smaller than sensors reported in [3, 4], our feasibility studies indicate the possibility to further scale down by at least one order of magnitude. These form factors are only possible in highly integrated processes; we have thus implemented a fully electromagnetic approach, allowing for use of advanced CMOS VLSI technologies for scalable, high-throughput production.
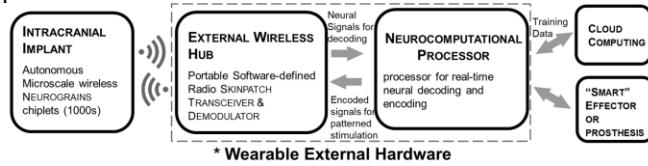

Figure 1. Concept graphic for an implantable Neurograin System comprising wireless microscale electronic sensors, wearable radio telecommunications hub and computational processor (described elsewhere [5]).

The major components of the neurograin system are illustrated in concept Fig. 1. At the core of the neurograin implant is an Application-Specific Integrated Circuit (ASIC), designed in 65 nm mixed-signal low-power process. This 0.25 mm² chip integrates analog, digital and RF circuitry allowing for autonomous operation, and can thus be deployed independently into the brain. Networked chip telecommunications are coordinated by a wearable external software-defined-radio (SDR). The latter has a field-programmable-gate-array (FPGA) back-end, which is utilized to provide real-time wireless demodulation, as well as neural decoding/encoding for closed-loop control. This neurocomputational processor is implemented to seamlessly access resources such as cloud computing for model optimization such as example, machine learning techniques.

The neurograin chiplets implement an on-chip multi-turn microcoil along with RF rectifiers and backscatter modulators which are described in [6]. Other salient features of the implantable chiplets and the full implant system are outlined in the sections below:

A. Ultra-Compact, Low power Analog-Front-End (AFE)

Sensing neural activity with high-fidelity is a critical requirement for the wireless neurograin sensors. We have implemented a self-standing, DC-coupled AFE with a merged amp-ADC architecture. By combining a chopping V/I converter, a VCO-based ADC and a mixed-signal differential electrode offset (DEO) canceling servo loop (Fig. 2a), we have eliminated capacitor use, leading both to large area savings and elimination of kT/C noise. The AFE is designed for ECoG signals, with a bandwidth of 500 Hz and a dynamic range of ± 1 mV (where the latter is adequate for differential signals from neurograin electrodes with an inter-electrode spacing of ~ 100 μm). The DC-offset cancellation range is ± 50mV, with 3.2 μW of power consumption from a 0.6 V supply. Input-referred noise is 2.2 μVrms over 500 Hz bandwidth for this implementation, which occupies 0.01 mm².

B. Wireless Telecommunications and Networking

Neurograin chiplets have a unique on-chip ID, which is derived from utilizing CMOS process variations [7]. This ID (discoverable during chip calibration) is used to queue neurograin nodes for a TDMA telecommunication network. The uplink telemetry uses Binary Phase Shift Keying (BPSK)-modulated RF backscatter at 10 Mbps, while the downlink employs amplitude-shift-keying based pulse-width-modulation (ASK-PWM) at 1 Mbps. The same wireless link is used for both power and telecoms, and the full network design relies on synchronized bidirectional communication for efficient link bandwidth usage (Fig. 2b), accommodating up to 1000 broadband ECoG neurograins on a single RF channel. We have also implemented in parallel a non-synchronized, periodic, packetized uplink-only TDMA network, which utilizes link bandwidth less efficiently and may suffer from occasional data collisions, but nonetheless provides an effective way to rapidly test small networks with fewer than 100 nodes such as the one described in this work.
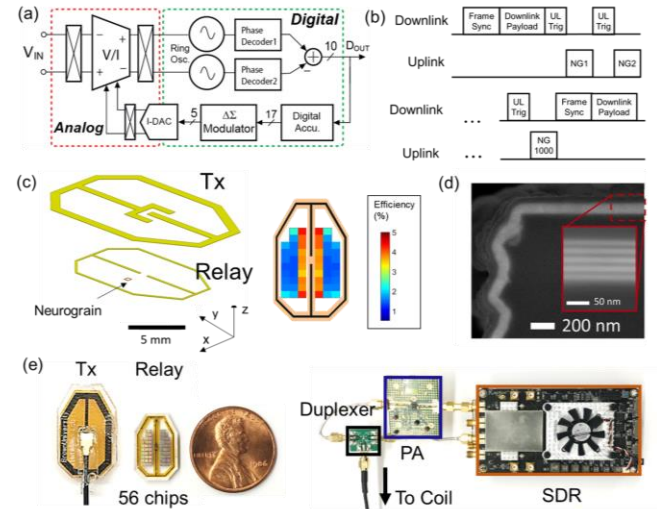

Figure 2. Major components of the neurograin system; (a) Schematic overview of an ultra-compact, low-noise AFE; (b) Synchronized bidirectional wireless TDMA network; (c) Tx and relay coil geometries and power-transfer efficiencies for a rodent-coil-system; (d) Edge cross-section of a hermetically encapsulated neurograin, demonstrating stacked-multilayer ALD coatings [8]; and (e) Rodent implant and coil-system (left) and external RF-hub (right).

C. Wireless Energy Harvesting

The neurograin implants are wirelessly powered in the near-field inductive coupling regime at ~ 1 GHz. The power budget for an individual neurograin is ~40 μW, and this must be harvested across a transcranial distance of 1 cm. We accomplish this by the introduction of a relay coil which has moderate coupling both with the external Tx and the neurograin microRx coils, thus increasing the efficiency of wireless power transfer at least 50x over a standard 2-coil approach. Furthermore, both the Tx and relay coils are designed with a double coil layout architecture, which creates a uniform magnetic field over a large plane enabling us to

capture a large number of spatially distributed neurograin microdevices with a single Tx-relay pair. One example is a 4-quadrant coil design covering a 2 cm x 2 cm area for a 1000 channel human implant, as described in [9]. Coil geometries are further adapted to accommodate anatomical variations, with Fig. 2c highlighting a custom design for *in vivo* rodent tests.

D. Neurograin Post-processing and Packaging

Chronic biocompatibility of the neural implant is a consideration of utmost importance for clinical viability. A robust physical electrode-tissue interface is a major aspect of this challenge along with hermetic packaging of the implant. We utilize standard post-process microfabrication techniques for patterned deposition of gold on top of the fabricated chiplet pads to form neurograin recording electrodes with impedances in the 100 kΩ range. We have also concurrently developed techniques for ALD-based stacked multilayer conformal coatings (Fig. 2d) for neurograin hermetic packaging [8]. The overall thickness profile of the packaging material is 100 nm, and packaged chiplets have been tested in an accelerated aging testbed with demonstrated viability well over 10 years at this time.

E. RF-back End & Data Processing

We use a compact SDR platform consisting of an Analog Devices AD9361 RF transceiver and a Zynq UltraScale+ system-on-chip (SoC) as the external telecommunications hub (Fig. 2e). The SDR is used to provide an RF transmission tone at 915 MHz (which is amplified using an IC-based power amplifier) for powering neurograins. The receive pathway on the SDR is fed by a duplexer (D5DA942M5K2S2) allowing for isolation of the BPSK-modulated data lobe. The SDR receiver front-end provides signal amplification, I/Q demodulation, and digitization at 45 MSa/s. The digitized IQ data may then either be ported to a PC for offline processing (in MATLAB/Simulink), or processed in real time using the Zynq FPGA (implementing HDL-optimized versions of the Simulink phase and sample timing recovery algorithms prior to BPSK demodulation).

III. BENCHTOP TESTING AND VALIDATION

A. AFE Validation

The fabricated AFE showed input impedance greater than 500 MΩ due to the DC-coupling. Fig. 3a shows the measured the output power spectral density (PSD) of the AFE with a 40 Hz sinusoid of 2 mV$_{pp}$, and shows SNDR of 51 dB and an SFDR of 62 dB. The AFE was also integrated with wireless RF circuitry and its functionality was validated after post-processing and packaging. The packaged chip was immersed in PBS and wirelessly powered with 3-coil wireless power and data link (WPDL). A concentric platinum-iridium oxide electrode was used to inject pre-recorded EEG data into PBS via an arbitrary waveform generator [10]. A standard extracellular plantinum recording electrode was concurrently used for reference voltage measurement with an operational amplifier. Fig. 3b shows recorded data from neurograin chiplets vs wired electrode where two traces overlay each other. This shows that the AFE on neurograins can robustly record local electric field changes over time confirming the functionality of the fully wireless recording system.
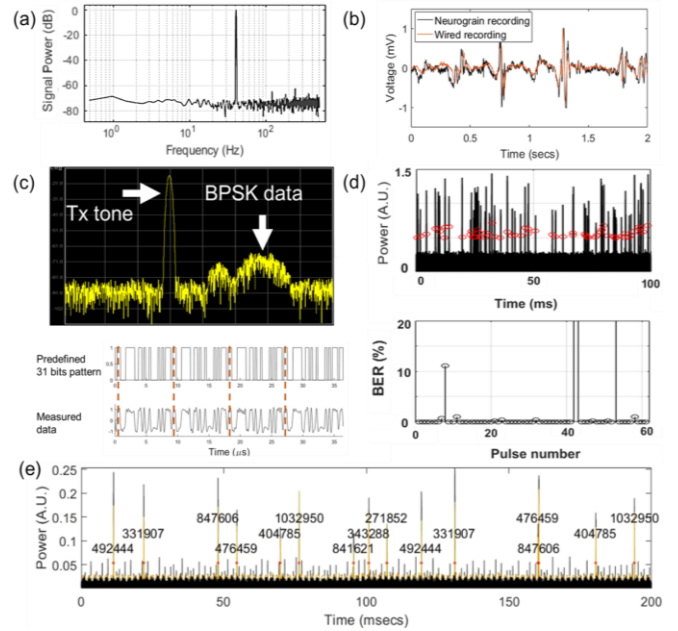

Figure 3. (a) The PSD of the front-end ADC with a 40 Hz sinusoid of 2 mV$_{pp}$, (b) EEG signal recording on saline with wired electrode and wireless neurograin, (c) Continuous BPSK backscattering spectrum of predefined 31 bits BPSK, (d) Periodic backscattering of 31 bits and BER at each pulse. (e) Fully wireless neurograin networking using 24 bits PUF address.

B. Wireless Energy Transfer & Networking

Since methods using wired microprobes can hinder the accurate measurement of WPDL capabilities of the neurograin micro-coil, we developed a fully wireless test bench to evaluate the WPDL fidelity. Two types of prototype chip were designed for this purpose: both generate a predefined 31-bits pattern, which is BSPK-modulated and transmitted either continuously or periodically. Continuous BPSK backscattering spectrum is evident as sidebands with separation matching the ASIC local oscillator frequency, e.g. 30 MHz, offset from the Tx tone as shown in Fig 3c. With this chip and RF front-end setup, we are able to achieve a high signal to noise ratio and demodulate the bit sequence with a consistent 0% bit error rate (BER) over 2000 cycles. The periodic BPSK ASIC offers a way to communicate with multiple chips through the TDMA protocol (Fig. 3d). Detecting and demodulating each 100 µs pulse can yield individual chip clock frequency estimates and data link BER. We placed and powered 64 chips in a single relay coil. Sixty-one pulses are detected in a 100 ms window (due to clock variability), and only 4 pulses show > 1 % BER (Fig 3d), where the latter is due to data collisions because of the choice of the unsynchronized TDMA telecom scheme.

After validating the network fidelity, the fully wireless recording neurograin which also utilizes unsynchronized TDMA protocol for multi-channel networking and AFE data transmission was characterized. In this chip, each data packet consists of a 32 bit predefined SYNC, 24 bit PUF address, 800 bit ADC data (100 sample) and 8 bit cyclic redundancy check (CRC). This packet structure allows the RF telecom hub to track and isolate individual recording channels on each neurograin. Fig. 3e shows the backscattering pulses from 8 neurograins and their PUF addresses where 8 different addresses are repeated every 100 ms. This benchtop testing validates neurograin's sensing and networking capacity and

the long-term robustness of wireless connection between the neurograin and the RF hub.

IV. Ex Vivo and In Vivo Assessment

A. Brain Slice Recording

Physiological validation of recording performance of a neurograin array has been assessed on Gfap Cre x ChR2YFP mouse brain slices while monitoring a seizure activity. 250-um thick mouse brain slices were prepared and transferred to an immersion chamber which is continuously perfused with artificial CSF (ACSF). The wireless 3-coil system is integrated into the bottom layer of the chamber. While recording the local field potential (LFP) of the slice with a wired single electrode placed above the brain slice, current stimulation is applied to the slice while the neurograin array was powered on to record field potentials from the bottom side of the slice. Recordings from the slices prior to seizure induction show characteristic slow LFP responses to electrical stimulation. Stimulation pulses are 350 µA in amplitude, 100 µs in width and applied at a rate of 40 Hz for 500 ms. After each stimulation event, a 10 to 20 ms long negative wave response was observed on the standard recording electrode. Multiple channels of the neurograin recorded a similar negative LFP response after stimulation, demonstrating the spatial spread of the effects of stimulation pulses (Fig. 4b). Subsequently, we used picrotoxin to induce epileptiform activity in the brain slice followed by electrical stimulation, where the latter was now able to evoke a seizure in the brain slice which was recorded by a proximate neurograin. Fig. 4c shows the seizure activity with preictal discharges and rhythmic bursts while Fig. 4d shows the development of seizure in the spectral domain. These results validate the AFE's recording of physiological signals and TDMA networking fidelity over the long period of time.
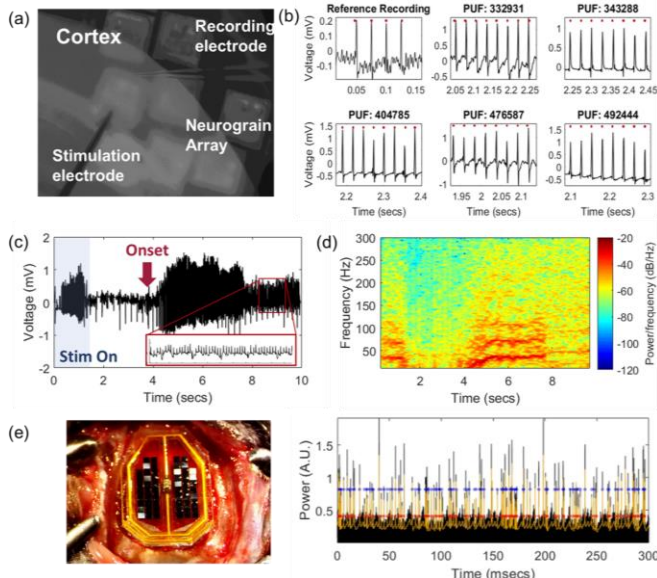

Figure 4. *In vitro* and *in vivo* demonstration of the neurograin system: (a) Brain slice recording setup, (b) Spatially-distributed field response recording from neurograin. The red dot shows electrical stimulation, (c) and (d) show results of seizure monitoring over 10 seconds, (e) In vivo implantation of 56 neurograin arrays and networking on the rat cortex. The red dot shows a pulse detection and the blue dot shows pulses with 32 bits SYNC.

B. In Vivo Demonstration

To demonstrate performance of the neurograins *in vivo*, spontaneous neural activity in rat cortex was monitored with a 56-neurograin array. A wild-type Long-Evans Rat was anesthetized with 3 % isoflurane and a bilateral craniotomy was made. After making the craniotomy, isoflurane was discontinued and ketamine/xylazine (80 and 5 mg/kg) was administered. The neurgrain array and relay coil were encapsulated with PDMS and placed above the cortex while the Tx coil transferred power from the top. Even with the dielectric surrounding the rat cortex tissue, we were able to communicate with 56 chips and observed 136 pulses within 300 ms. Among those pulses, we detected the predefined 32 bit SYNC from 118 pulses (the occasional collision of pulses sometimes impedes SYNC data detection). The correlation study between an external stimulus and *in vivo* extracellular recording from neurograin array has not been done yet. Further experiments will include sensory stimulations to monitor the event-related sensory evoked potential.

V. Summary/Future Directions

We have designed and validated the performance of a wireless, spatially-distributed, autonomous microscale "Neurograin" sensor network in *ex vivo* brain slices and *in vivo* rat models. These are the first steps toward the long-term development of the comprehensive system (Fig. 1). Ongoing work is focusing on incorporating TDMA synchronization through use of downlink telemetry, testing of a stimulating neurograin ASIC, and integration of a neurocomputational processor to yield next-generation implantable/wearable neural interfaces with 1000s of sensor nodes.

References

[1] L. R. Hochberg, M. D. Serruya, G. M. Friehs, J. A. Mukand, ... and J. P. Donoghue, "Neuronal ensemble control of prosthetic devices by a human with tetraplegia," *Nature*, vol. 442, pp. 164–171, 2006.

[2] D. A. Borton, M. Yin, J. Aceros, and A.V. Nurmikko, "An implantable wireless neural interface for recording cortical circuit dynamics in moving primates," *Journal of neural engineering*, vol. 10(2), 2013.

[3] D. Seo, R. M. Neely, K. Shen, U. Singhal, J. M. Rabaey, ... and M. M. Maharbiz, "Wireless recording in the peripheral nervous system with ultrasonic neural dust," *Neuron*, vol 91(3), pp. 529-539, 2016.

[4] P. Yeon, M. S. Bakir, and M. Ghovanloo, "Towards a 1.1 mm 2 free-floating wireless implantable neural recording SoC," In Custom Integrated Circuits Conference, IEEE, pp. 1-4, 2018.

[5] C. Heelan, A. V. Nurmikko and W. Truccolo, "FPGA implementation of deep-learning recurrent neural networks with sub-millisecond real-time latency for BCI-decoding of large-scale neural sensors (104 nodes)," *EMBC*, pp. 1070-1073, 2018.

[6] V. W. Leung, J. Lee, S. Li, S. Yu, C. Kilfovle, L. Larson, ... and F. Laiwalla, "A CMOS Distributed Sensor System for High-Density Wireless Neural Implants for Brain-Machine Interfaces. *IEEE 44th European Solid State Circuits Conference,* IEEE, pp. 230-233, 2018.

[7] G. E. Suh, and S. Devadas, "Physical unclonable functions for device authentication and secret key generation," *In Design Automation Conference, IEEE,* pp. 9-14, 2007.

[8] J. Jeong, F. Laiwalla, J. Lee, R. Ritasalo, M. Pudas, L. Larson, V. Leung, A. Nurmikko, "Conformal Hermetic Sealing of Wireless Microelectronic Implantable Chiplets by Multilayered Atomic Layer Deposition (ALD)," *Adv. Funct. Mater*, 13 Dec 2018, 1806440.

[9] J. Lee, F. Laiwalla, … and A. Nurmikko, "Wireless power and data Link for ensembles of sub-mm scale implantable sensors near 1GHz," In *Biomedical Circuits and Systems Conference,* IEEE, 2018 (in press).

[10] R. G. Andrzejak et al., "Nonrandomness, nonlinear dependence, and nonstationarity of electroencephalographic recordings from epilepsy patients," *Physical Review E*, vol. 86(4), 2012.